# CHAPTER 4

# GENERAL ASPECTS OF MUTUAL ADMITTANCE OF CPW-FED TWIN SLOTS ON CONDUCTOR-BACKED TWO-LAYER SUBSTRATES

## 4.1 INTRODUCTORY REMARKS

The present chapter is concerned with an exploratory investigation of the mutual admittance between identical (twin) CPW-fed slots on a single-layer substrate with a conducting back plane placed at a distance $h_2$ from the dielectric side of the substrate (the substrate can also be thought of as a conductor-backed two-layer substrate with an air bottom layer). While mutual coupling has been characterized to a greater or lesser extent for a number of kinds of slots on layered media including centre-fed rectangular slots on a dielectric half-space [57] and CPW-fed slots on two- and three-layer substrates without conductor backing [38], it has not yet, to the knowledge of the author, been done for CPW-fed slots on two-layer parallel-plate substrates. Fig. 4.1 shows a broadside twin slot configuration.[1]

Two separate issues are addressed, namely a characterization of the mutual admittance between twin slots with half-lengths in the vicinity of the first-resonance and second-resonance half-lengths of the corresponding isolated slots (Section 4.2), and an investigation of the effect of back plane distance on mutual coupling (Section 4.3).[2] Since each of Sections 4.2 and 4.3 are essentially self-contained, their respective conclusions sections (*i.e.*, Sections 4.2.5 and 4.3.4) replace the customary concluding section to the chapter.

[1] This configuration is similar to that of Fig. 3.1.
[2] A distinction is made between mutual admittance and mutual coupling that will be explained in the course of the chapter.

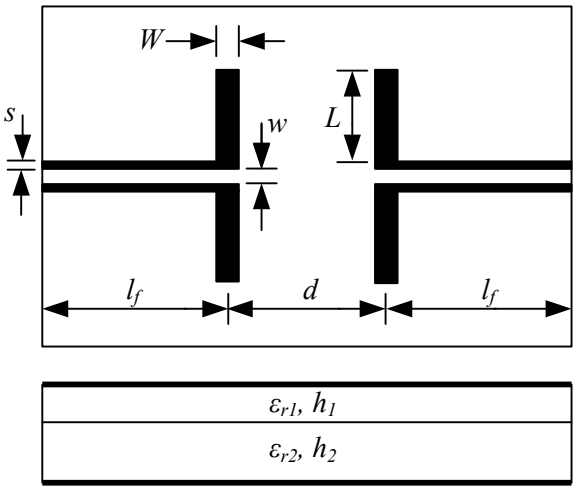


FIGURE 4.1: Top and side views of broadside CPW-fed twin slot antennas on conductor-backed two-layer substrate. $L \equiv$ half-length and $W \equiv$ width of radiating slots; $d \equiv$ distance between radiating slots; $s \equiv$ slot width and $w \equiv$ centre strip width of feed lines; $l_f \equiv$ length of feed lines; $h_1$ and $h_2 \equiv$ dielectric layer heights; $\epsilon_{r1}$ and $\epsilon_{r2} \equiv$ relative dielectric constants.

## 4.2 MUTUAL ADMITTANCE OF FIRST- AND SECOND-RESONANCE CPW-FED TWIN SLOTS ON CONDUCTOR-BACKED TWO-LAYER SUBSTRATE

### 4.2.1 Introduction

The aim of this section is to provide a more comprehensive characterization of the mutual admittance between CPW-fed slots on a conductor-backed two-layer substrate than is currently available. The characterization takes the form of curves for the mutual admittance between first-resonance twin slots and second-resonance twin slots as a function of separation distance along standard paths. Similar data is available for, *e.g.*, slots on semi-infinite substrates [57], first-resonance rectangular slots in the broad wall of rectangular waveguide [58], and first-resonance narrow center-fed slots on an infinite ground plane radiating in a homogeneous free space (graphs for the mutual impedance between the dual slender electric dipoles are well known and can be found in standard texts [18, Fig. 7.24], [59, Fig. 7.8]). In [57], the authors suggest that data of this nature can be used in the design of slot arrays using a first-order multi-port mutual admittance approach, where the array multi-port mutual admittance matrix is obtained by considering individual pairs of slots at a time (*cf.* Chapter 1). The mutual admittance curves for CPW-fed first- and second-resonance twin slots on a conductor-backed two-layer substrate presented in this chapter will be compared to findings relating to certain of the above types of slots. In the course of the investigation, the nature of first- and second-resonance slot electric field distributions will be addressed.

### 4.2.2 Method

Mutual admittance curves were computed using the moment-method-based electromagnetic simulator IE3D [60], which made it possible to explicitly account for feed line effects. Details of experimental results that verify the accuracy of IE3D with respect to mutual admittance computations involving CPW-fed slots on two-layer parallel-plate substrates are given in Sections 4.3 and 5.4.2.5.

The two-layer parallel-plate substrate and CPW feed lines were designed as follows. Relative dielectric constants $\epsilon_{r1}$ and $\epsilon_{r2}$ were 3.38 and 1 respectively, with substrate layer heights $h_1 = 0.813$ mm and $h_2 = 5$ mm; $h_2$ equals $\lambda_0/6$ at the 10 GHz simulation frequency, with $\lambda_0$ the free-space wavelength (the substrate was used in an earlier successful implementation of an 8-element uniform linear CPW-fed array [36]). A higher dielectric constant has to be chosen for the top substrate layer than for the bottom layer in order to help achieve a non-leaky CPW transmission line [12]. At 10 GHz, the only substrate mode that could propagate was the the $TM_0$ mode. A CPW centre strip width $w = 3.7$ mm and slot width $s = 0.2$ mm yielded a characteristic impedance of about 50 Ω.

Twin slot dimensions used in mutual admittance calculations were determined as follows.

First, an isolated CPW-fed radiating slot with a width $W = 0.4$ mm was designed to be resonant at 10 GHz by appropriately adjusting its half-length $L$. Half-lengths corresponding to the first and second resonances were $L_{res,1} = 0.27\lambda_s = 5.7$ mm and $L_{res,2} = 0.52\lambda_s = 10.87$ mm respectively ($\lambda_s$ is the wavelength at 10 GHz of a 0.4 mm wide slotline on the two-layer parallel-plate substrate described above). $L_{res,1}$ and $L_{res,2}$ corresponded to resonant self-impedances of about 420 Ω and 14 Ω respectively.

Subsequently, mutual admittance $Y_{12}$ against distance $d$ was computed for two sets of twin slots based on the above isolated slots. Slot half-lengths for the first set were in the vicinity of $L_{res,1}$, while half-lengths for the second set were in the vicinity of $L_{res,2}$; in all cases $W$ was 0.4 mm. Two slot configurations were investigated, namely broadside (*cf.* Fig. 4.1), and collinear. Throughout, lengths $l_f$ of feed lines were $0.5\lambda_{CPW}$, where $\lambda_{CPW}$ is the CPW wavelength at 10 GHz, in effect referring two-port network parameters to the centres of radiating slots.

For purposes of comparison, the mutual admittance between a set of identical broadside narrow rectangular slots in an infinite ground plane was computed against slot separation. Slot lengths $2l$ were in the vicinity of half a free-space wavelength corresponding to slots operating around their first resonances. Expressions for the mutual impedance $Z_{12}^d$ between broadside slender electric dipoles

in free space, assuming sinusoidal current distributions, are available [18, Eqs. (7.155) and (7.156)]. The mutual admittance $Y_{12} = G_{12} + jB_{12}$ between the complementary centre-fed narrow slots in an infinite ground plane can be found from the former expressions using Booker's relation, $Y_{12} = (4/\eta_0^2)Z_{12}^d$, where $\eta_0$ is the intrinsic impedance of free space. The resulting graphs for identical broadside slots of length $2l$ are shown in Figs. 4.2 ($G_{12}$) and 4.3 ($B_{12}$); curves for $2l$ values of $0.375\lambda_0$, $0.5\lambda_0$ and $0.625\lambda_0$ are shown.

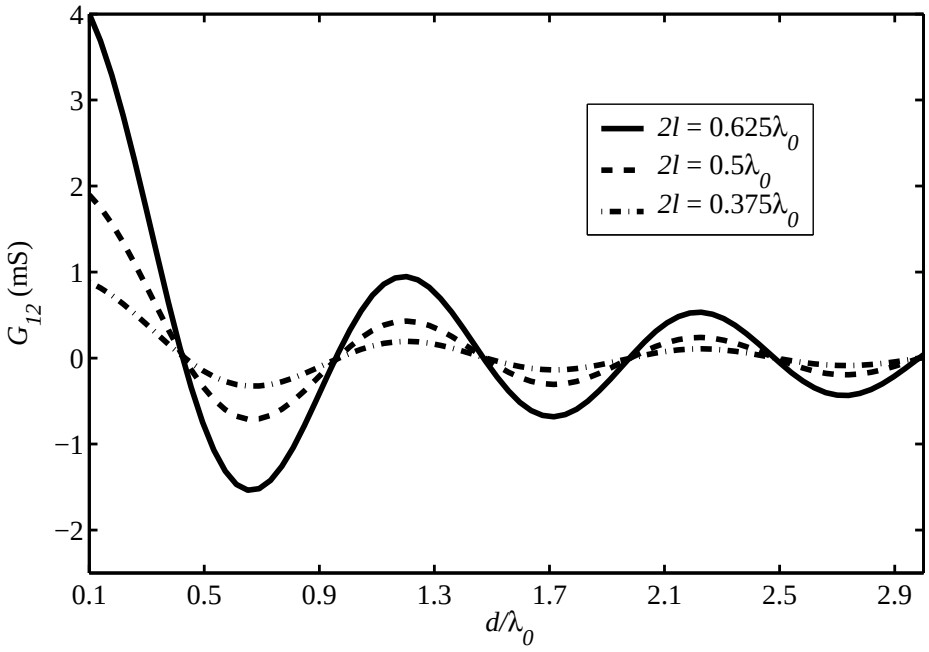


FIGURE 4.2: Mutual conductance $G_{12}$ between identical centre-fed broadside narrow slots in an infinite ground plane against slot separation $d/\lambda_0$. The medium is homogeneous free space.

### 4.2.3 Mutual admittance between broadside slots

Figs. 4.4 and 4.5 show the magnitude and phase of the $\hat{y}$-directed aperture electric field along the centre of the isolated *first-resonance* slot which had $W = 0.4$ mm and $L = L_{res,1} = 0.27\lambda_s$ mm; the $\hat{x}$-directed field component can be considered negligible compared to the $\hat{y}$-component and is not shown (see Fig. 4.6 for coordinate axes). Fields for slots with half-lengths $0.9L_{res,1}$ and $1.1L_{res,1}$ are also shown. As expected, in all cases the field magnitude is approximately half-cosinusoidal while the phase is nearly constant. This is similar to electric currents on centre-fed cylindrical dipoles of comparable electrical lengths [18, Figs. 7.6 and 7.7]. Fig. 4.5 indicates that a change in slot half-length results in a phase that is offset with respect to the previous length's phase.

Plots of mutual admittance $Y_{12}$ against broadside distance $d/\lambda_{CPW}$ between twin slots with the above half-lengths are given in Fig. 4.7. The range of $d$ was chosen as $0.9\lambda_{CPW} \leq d \leq 3\lambda_{CPW}$,

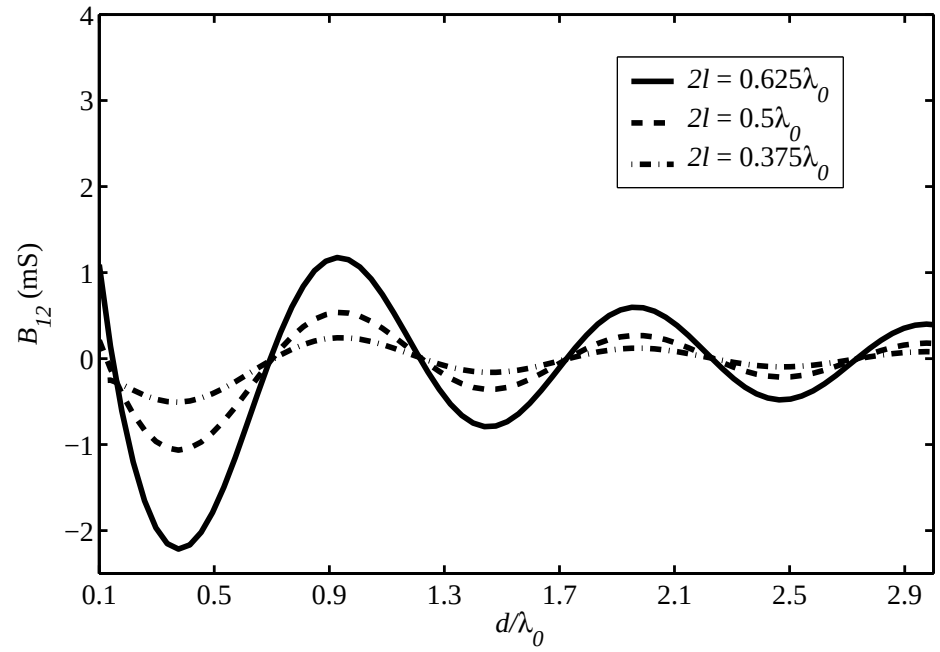


FIGURE 4.3: Mutual susceptance $B_{12}$ between identical centre-fed broadside narrow slots in an infinite ground plane against slot separation $d/\lambda_0$. The medium is homogeneous free space.

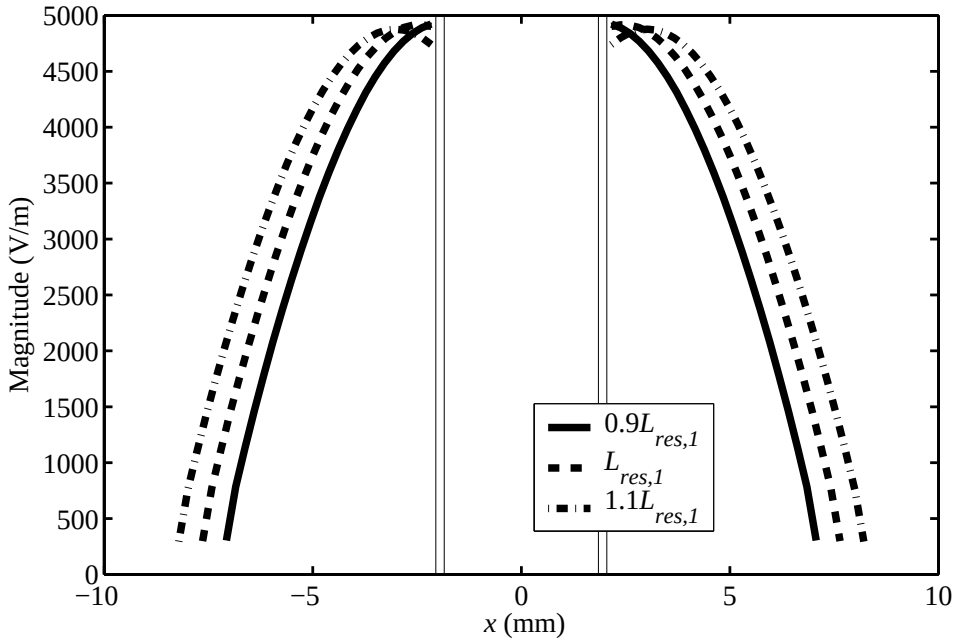


FIGURE 4.4: Magnitude of electric field of isolated slots with half-lengths in vicinity of first-resonance half-length $L_{res,1}$ on two-layer parallel-plate substrate. $L_{res,1} = 0.27\lambda_s = 5.7$ mm; $W = 0.4$ mm; $h_1 = 0.813$ mm; $h_2 = 5$ mm; $\epsilon_{r1} = 3.38$; $\epsilon_{r2} = 1$. Vertical lines correspond to positions of CPW slots.

given that mutual coupling in linear arrays with slots spaced $\lambda_{CPW}$ apart has been taken into account for inter-slot spacings of up to $3\lambda_{CPW}$ [35]. The figure suggests that $|Y_{12}|$ increases as slot length increases, as in the case of centre-fed slots in an infinite ground plane (Figs. 4.2 and 4.3).

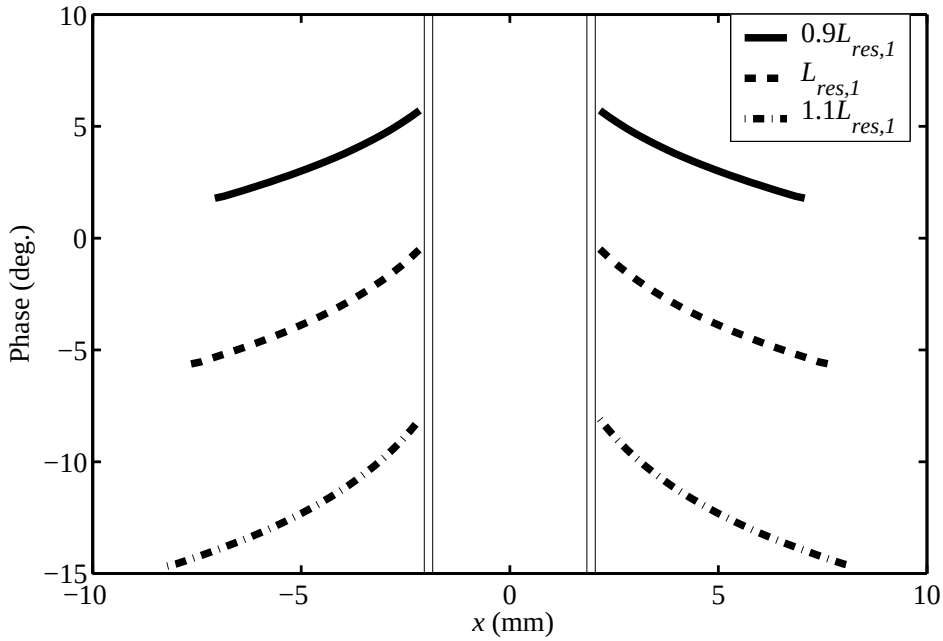


FIGURE 4.5: Phase of electric field of isolated slots with half-lengths in vicinity of first-resonance half-length $L_{res,1}$ on two-layer parallel-plate substrate. $L_{res,1} = 0.27\lambda_s = 5.7$ mm; $W = 0.4$ mm; $h_1 = 0.813$ mm; $h_2 = 5$ mm; $\epsilon_{r1} = 3.38$; $\epsilon_{r2} = 1$. Vertical lines correspond to positions of CPW slots.

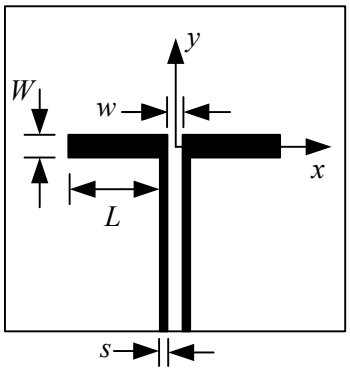


FIGURE 4.6: Orientation of coordinate system with respect to CPW-fed slot. The $z$-axis points out of the page.

Fig. 4.8 shows a plot of the magnitude of the normalized mutual admittance $y_{12}$ against distance $d/\lambda_{CPW}$; $y_{12}$ is the mutual admittance $Y_{12}$ normalized to the magnitude of the relevant isolated slot self-admittance. The relative size of the mutual admittance magnitudes with respect to the slots' self-admittance magnitudes is an indicator of the extent of coupling between the slots. Fig. 4.8 indicates that mutual coupling is the greatest for the slots with $L = L_{res,1}$.

Since *second-resonance* slots have self-impedances that lie on relatively stationary (*i.e.*, "flat")

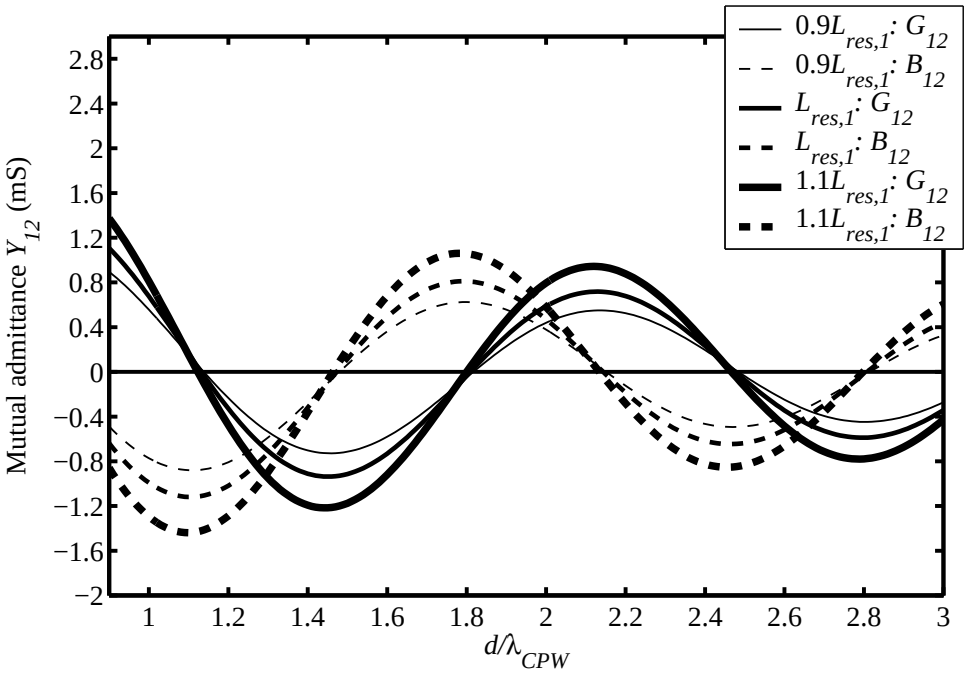


FIGURE 4.7: Mutual admittance between identical CPW-fed slots against broadside distance $d/\lambda_{CPW}$ at 10 GHz on a two-layer parallel-plate substrate. Computations were performed for slot half-lengths in the vicinity of that of a first-resonant isolated slot. $W = 0.4$ mm; $h_1 = 0.813$ mm; $h_2 = 5$ mm; $\epsilon_{r1} = 3.38$; $\epsilon_{r2} = 1$.

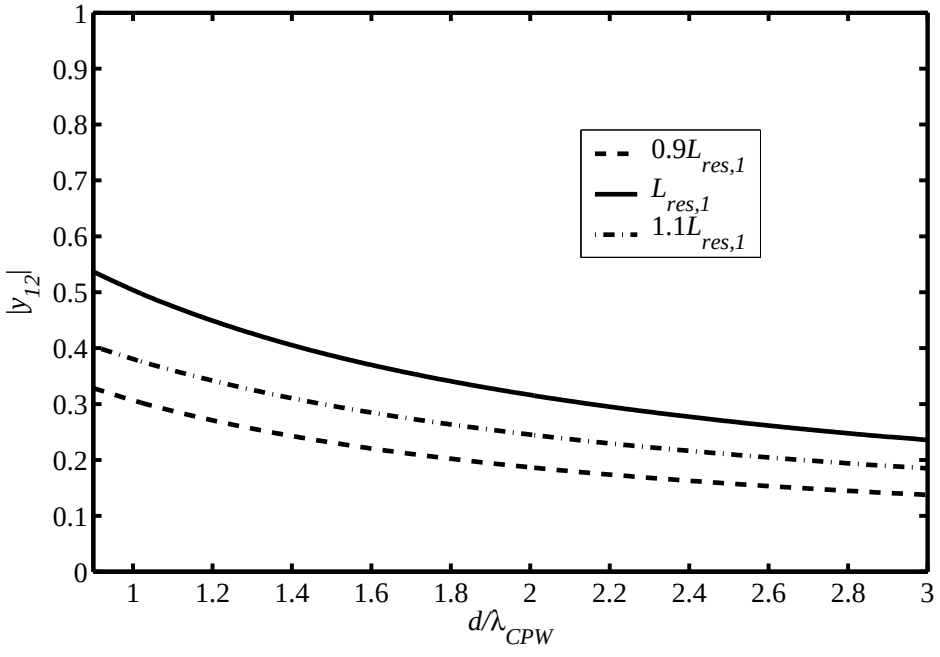


FIGURE 4.8: Magnitude of normalized mutual admittance between identical CPW-fed slots against broadside distance $d/\lambda_{CPW}$ at 10 GHz on a two-layer parallel-plate substrate. Computations were performed for slot half-lengths in the vicinity of that of a first-resonant isolated slot. $W = 0.4$ mm; $h_1 = 0.813$ mm; $h_2 = 5$ mm; $\epsilon_{r1} = 3.38$; $\epsilon_{r2} = 1$.

portions of their self-impedance-against-frequency curves (*cf.* Fig. 2.2), these slots are preferable to first-resonance slots for use in arrays [34]. Figs. 4.9 and 4.10 show the aperture electric field along the slot centre for the isolated second-resonance slot described above ($W = 0.4$ mm, $L = L_{res,2} = 0.52\lambda_s = 5.7$ mm), as well as the fields for slots with half-lengths close to $L_{res,2}$, namely $0.85L_{res,2}$, $0.95L_{res,2}$, and $1.1L_{res,2}$. Field magnitudes resemble the magnitude of a full cycle of a sinusoid. Phases, while changing little in the outer reaches of the slots, exhibit a sharp rise closer to the CPW feed line which becomes more apparent as slot length increases, leading into a $180^\circ$ phase reversal in the case of the $1.1L_{res,2}$ slot. Increases in slot length translate into phase offsets with respect to phases of preceding lengths. These results are similar to currents calculated for centre-fed cylindrical dipoles of comparable electrical lengths [18, Figs. 7.6 and 7.7].

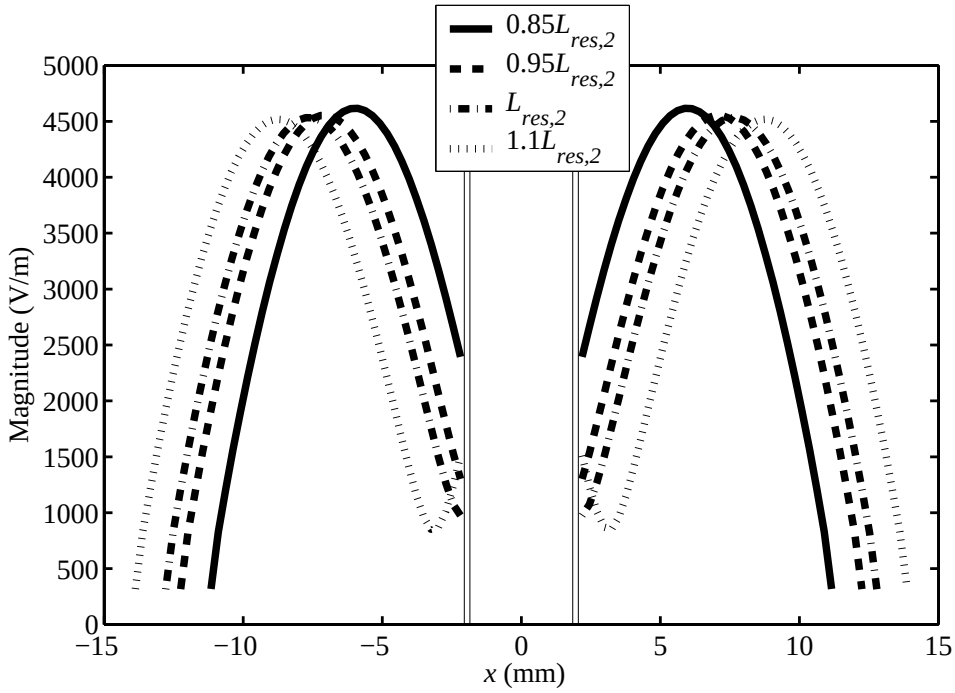


FIGURE 4.9: Magnitude of electric field of isolated slots with half-lengths in vicinity of second-resonance half-length on two-layer parallel-plate substrate. $L_{res,2} = 0.52\lambda_s = 10.87$ mm; $W = 0.4$ mm; $h_1 = 0.813$ mm; $h_2 = 5$ mm; $\epsilon_{r1} = 3.38$; $\epsilon_{r2} = 1$.

Figs. 4.11 and 4.12 show mutual conductance $G_{12}$ and mutual susceptance $B_{12}$ against broadside distance $d$ for slot half-lengths $0.85L_{res,2}$, $0.95L_{res,2}$, $L_{res,2}$, and $1.1L_{res,2}$. A number of observations can be made with respect to Figs. 4.11 and 4.12 in conjunction with Fig. 4.13, which gives the magnitude of the mutual admittance. First, the set of second-resonance curves in these figures are not as regular in shape as the first-resonance curves of Fig. 4.7. The effect is most apparent for the $L_{res,2}$ twin slots, the second most apparent for the $1.1L_{res,2}$ twin slots, and the least apparent for twin slots with $L < L_{res,2}$ to the extent of being virtually unobservable for the case

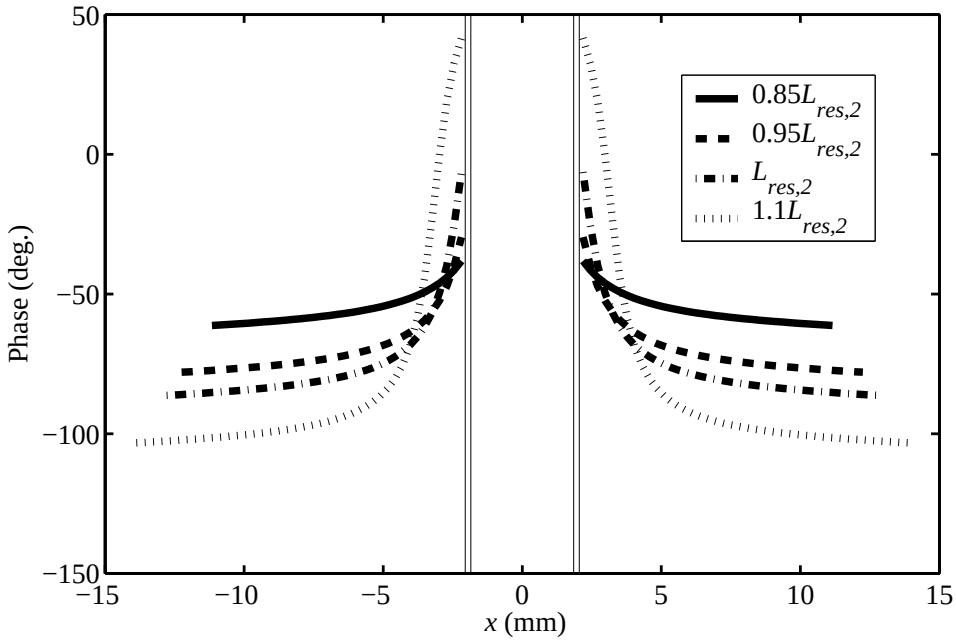


FIGURE 4.10: Phase of electric field of isolated slots with half-lengths in vicinity of second-resonance half-length on two-layer parallel-plate substrate. $L_{res,2} = 0.52\lambda_s = 10.87$ mm; $W$ = 0.4 mm; $h_1$ = 0.813 mm; $h_2$ = 5 mm; $\epsilon_{r1}$ = 3.38; $\epsilon_{r2}$ = 1.

$L = 0.85L_{res,2}$. Second, the magnitude of the mutual admittance is highest for the resonant slot half-length (*i.e.*, $L = L_{res,2}$), and decreases as $L$ increases or decreases as illustrated in Fig. 4.13. This is unlike the set of first-resonance curves, where the mutual admittance magnitude increases with increasing slot length. Third, the set of second-resonance mutual conductance curves are shifted with respect to each other; so are mutual susceptance curves. Thus a 5% decrease in $L_{res,2}$ results in a right shift of about $\lambda_{CPW}/5$ in the position of the first mutual conductance peak and a 10% increase in a left shift of about $\lambda_{CPW}/3$. This is unlike the curves in Fig. 4.7 for slots with half-lengths in the vicinity of $L_{res,1}$, and the curves for narrow centre-fed rectangular slots in an infinite ground plane. Here, changes in slot half-length have negligible influence on positions of maxima, minima and zero-crossings of conductance and susceptance curves that may be described as being "in phase". These shifts are probably linked to the fact that phases of second-resonance slot fields are not constant.

Fig. 4.14 shows a plot of the magnitude of the normalized mutual admittance $y_{12}$ against distance $d/\lambda_{CPW}$; $y_{12}$ is the mutual admittance $Y_{12}$ of Fig. 4.13 normalized to the magnitude of the relevant isolated slot self-admittance. This measure confirms that, on the whole, mutual coupling is greatest for the slots with $L = L_{res,2}$.[3]

[3] It is also possible to normalize $Y_{12}$ to the magnitude of the relevant two-port self-admittance $Y_{11}$ (*cf.* Fig. 5.46). This yielded a similar hierarchy of mutual coupling sizes, *i.e.*, largest for the case $L = L_{res,2}$ and smallest for $L = 0.85L_{res,2}$.

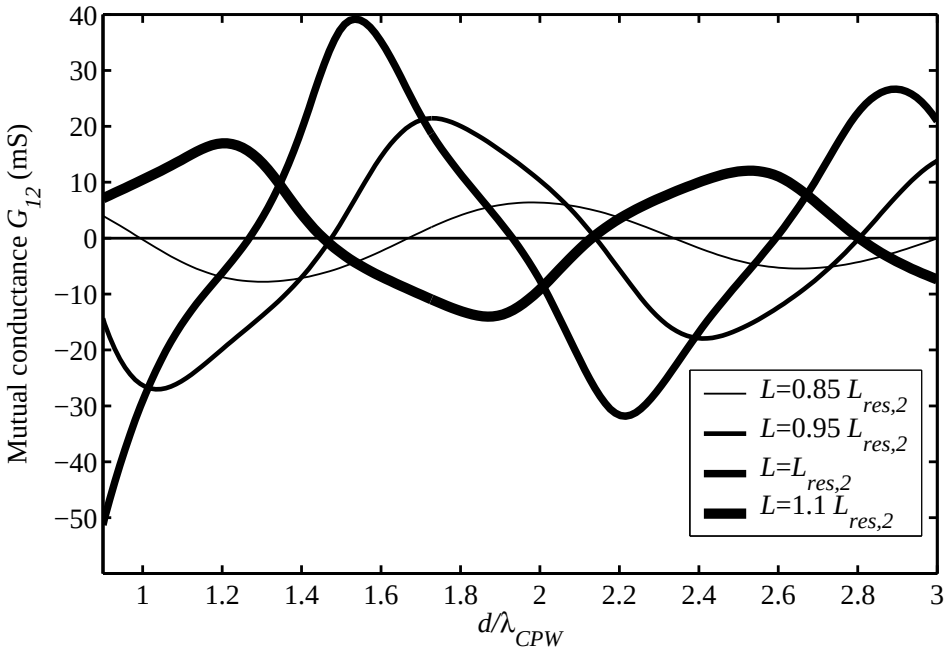


FIGURE 4.11: Mutual conductance between CPW-fed slots against broadside distance $d/\lambda_{CPW}$ at 10 GHz for slot half-lengths in the vicinity of $L_{res,2}$. $W$ = 0.4 mm; $h_1$ = 0.813 mm; $h_2$ = 5 mm; $\epsilon_{r1}$ = 3.38; $\epsilon_{r2}$ = 1.

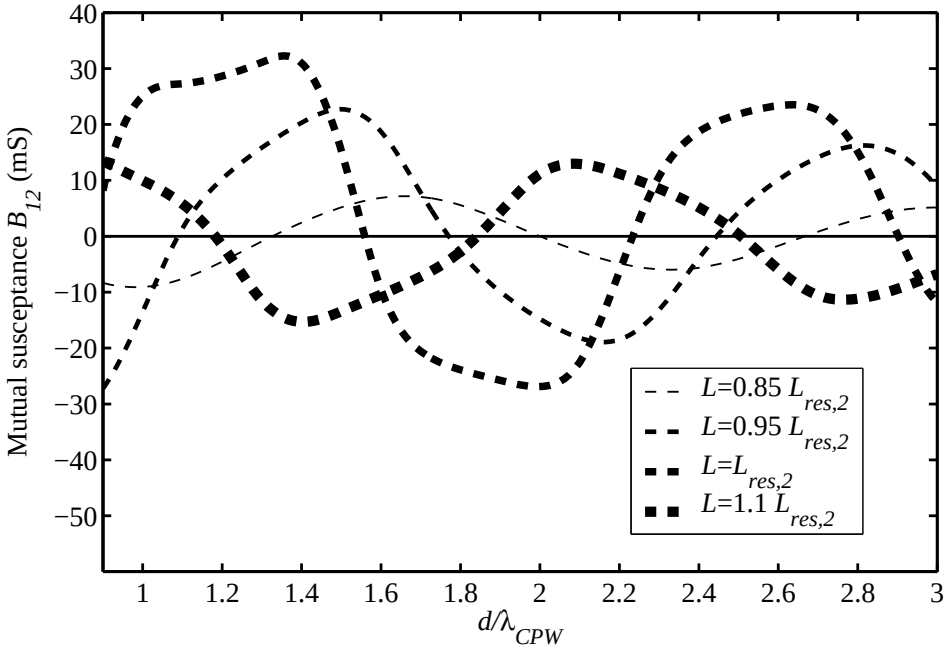


FIGURE 4.12: Mutual susceptance between CPW-fed slots against broadside distance $d/\lambda_{CPW}$ at 10 GHz for slot half-lengths in the vicinity of $L_{res,2}$. $W$ = 0.4 mm; $h_1$ = 0.813 mm; $h_2$ = 5 mm; $\epsilon_{r1}$ = 3.38; $\epsilon_{r2}$ = 1.

It is instructive to compare the relative magnitudes of the mutual admittance normalized to the magnitude of the relevant isolated slot self-admittance for slots at or close to resonance, namely $0.5\lambda_0$

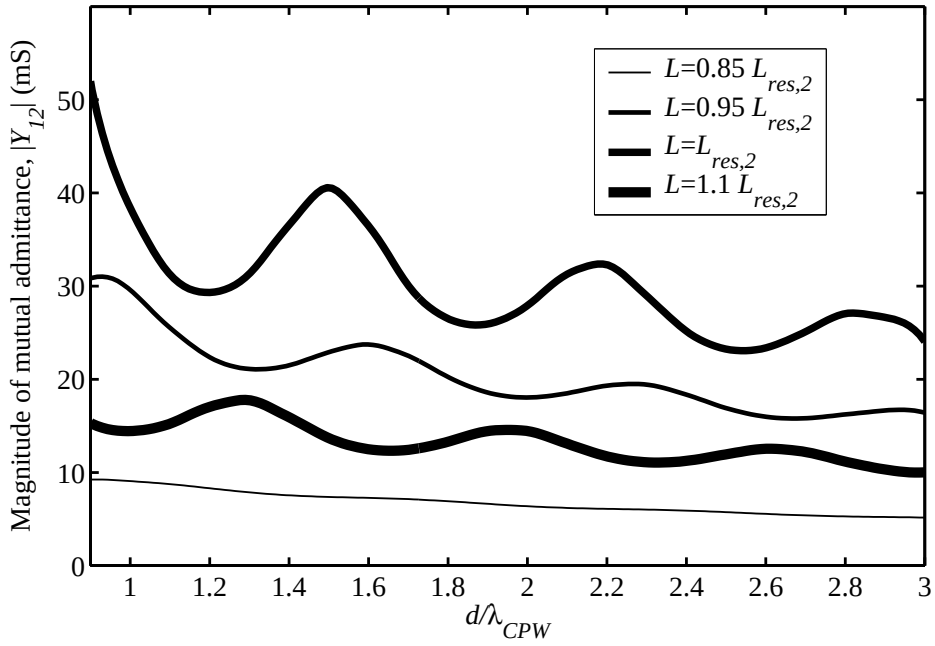


FIGURE 4.13: Magnitude of mutual admittance between CPW-fed twin slots against broadside distance $d/\lambda_{CPW}$ at 10 GHz for slot half-lengths in the vicinity of $L_{res,2}$. $W$ = 0.4 mm; $h_1$ = 0.813 mm; $h_2$ = 5 mm; $\epsilon_{r1}$ = 3.38; $\epsilon_{r2}$ = 1.

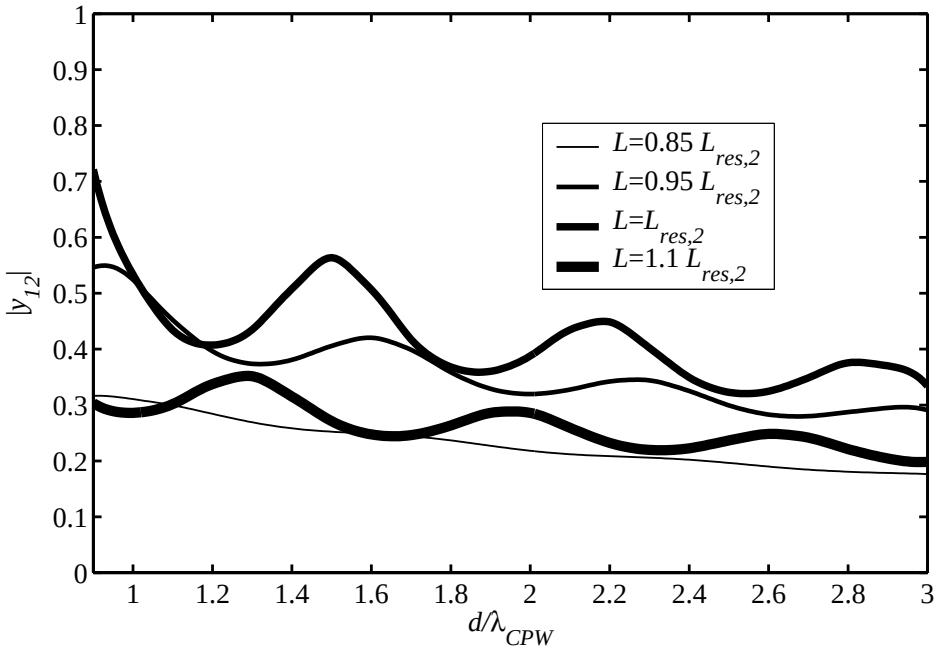


FIGURE 4.14: Magnitude of normalized mutual admittance between identical CPW-fed slots against broadside distance $d/\lambda_{CPW}$ at 10 GHz for slot half-lengths in the vicinity of $L_{res,2}$. $W = 0.4$ mm; $h_1 = 0.813$ mm; $h_2 = 5$ mm; $\epsilon_{r1} = 3.38$; $\epsilon_{r2} = 1$.

centre-fed rectangular slots in an infinite ground plane in free space, CPW-fed slots on a two-layer parallel-plate substrate with $L = L_{res,1}$, and CPW-fed slots on a two-layer parallel-plate substrate with $L = L_{res,2}$ (the inter-slot spacing range is physically the same as that of Figs. 4.7 and 4.11–4.14).

On the whole, the normalized mutual admittance magnitude is smallest for the infinite ground plane slots, and largest in the case of the CPW-fed slots with $L = L_{res,2}$, suggesting that the effect of coupling is smallest for $0.5\lambda_0$ infinite ground plane slots, and largest for the CPW-fed slots with $L = L_{res,2}$.

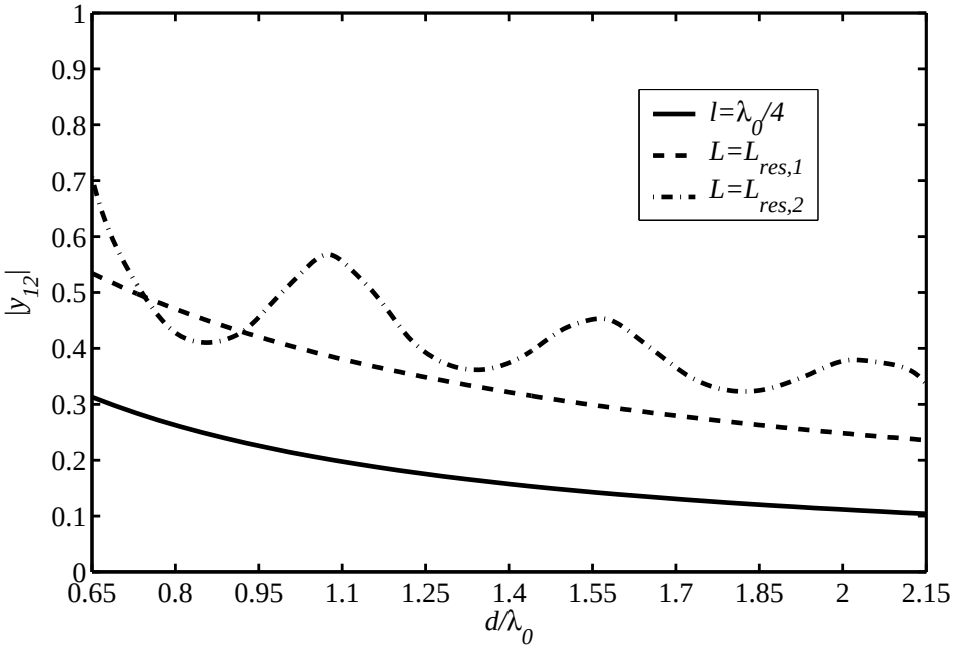


FIGURE 4.15: Magnitude of normalized mutual admittance, $|y_{12}|$, against slot separation $d/\lambda_0$ for identical centre-fed broadside narrow slots with length $2l = 0.5\lambda_0$ in infinite ground plane, and CPW-fed twin slots with $L = L_{res,1}$ and $L = L_{res,2}$ on conductor-backed two-layer substrate ($W = 0.4$ mm; $h_1 = 0.813$ mm; $h_2 = 5$ mm; $\epsilon_{r1} = 3.38$; $\epsilon_{r2} = 1$).

### 4.2.4 Mutual admittance between collinear slots

For the investigation of CPW-fed slots oriented in a collinear manner, two pairs of identical slots were considered. The first pair had $W = 0.4$ mm and $L = L_{res,2} = 0.52\lambda_s$, and the second pair $W = 0.4$ mm and $L = 1.1L_{res,2}$. The resulting mutual admittance curves are displayed in Fig. 4.16, with the largest mutual admittance values observed for the slots with $L = L_{res}$. As expected, mutual admittance on the whole was substantially less in the collinear direction; mutual coupling expressed as mutual admittance normalized to the magnitude of the relevant isolated slot self-admittance was in fact negligible compared to the broadside case. Positions of maxima and minima again showed relative shifts, contrary to the collinear curves for slender free-space dipoles in [18, Fig. 7.24], [59, Fig. 7.8]; curves however were regular in shape.

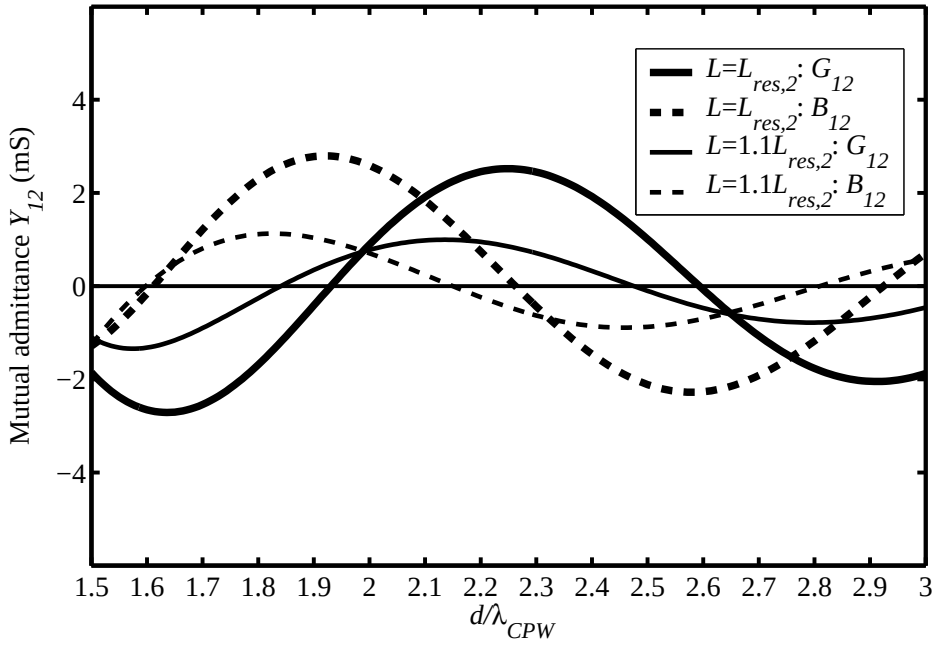


FIGURE 4.16: Mutual admittance between CPW-fed slots against collinear distance $d/\lambda_{CPW}$ at 10 GHz for slot half-lengths in the vicinity of $L_{res,2}$. $W$ = 0.4 mm; $h_1$ = 0.813 mm; $h_2$ = 5 mm; $\epsilon_{r1}$ = 3.38; $\epsilon_{r2}$ = 1.

### 4.2.5 Conclusions

A characterization of the mutual admittance between CPW-fed slots on a conductor-backed two-layer substrate, more comprehensive than had been available previously, was presented. The substrate allowed for propagation of the $TM_0$ surface-wave mode only. Mutual admittance between twin slots was computed using IE3D for a number of half-lengths in the vicinities of the first and second resonant half-lengths of the isolated slots as a function of slot separation along broadside and collinear paths; such data might be of use in the design of arrays in the manner suggested in [57]. Feed lines were $0.5\lambda_{CPW}$ long, in effect referring two-port network parameters to radiating slot centres. Mutual admittance curves for the set of broadside second-resonance twin slots were irregular in shape, and shifted with respect to each other, unlike the first-resonance curves that were similar in shape to mutual admittance curves for centre-fed narrow slots in an infinite ground plane. The irregularity was most marked for twin slots with $L = L_{res,2}$. Mutual coupling between broadside first-resonance CPW-fed twin slots and second-resonance CPW-fed twin slots on the two-layer parallel-plate substrate referred to the magnitude of the isolated slot self-admittance was greater than the mutual coupling between broadside $0.5\lambda_0$ centre-fed narrow rectangular slots in an infinite ground plane, with mutual coupling between the second-resonance CPW-fed slots greater than that between the first-resonance CPW-fed twin slots. Compared to the broadside case, mutual coupling between identical collinear slots with half-lengths in the vicinity of the second-resonance half-length was negligible.

## 4.3 EFFECT OF BACK PLANE DISTANCE ON MUTUAL ADMITTANCE BETWEEN CPW-FED SLOTS ON CONDUCTOR-BACKED TWO-LAYER SUBSTRATES

### 4.3.1 Introduction

In Chapter 3, the effect of back plane distance on radiation efficiency and impedance bandwidth of CPW-fed twin slots on a conductor-backed two-layer substrate with air bottom layer was explored (*cf.* Fig. 4.1). The present section investigates the effect of back plane distance on mutual coupling between CPW-fed twin slots on such a substrate.[4] For linear slot arrays on $\lambda_d$/4 substrates with a back reflector placed on the side of the CPW ground planes, it has been noted that a reflector distance of $\lambda_0$/4 has minimal effect on the antenna input impedance [34]. A question is whether for arrays on two-layer parallel-plate substrates, a bottom layer height $h_2$ of $\lambda_0$/4 would also result in a minimal effect on the array's input impedance; the question can be related to the extent of the influence of a back plane on internal coupling (*i.e.*, coupling on the dielectric side).

### 4.3.2 Numerical method

Numerical investigations were performed using IE3D [60]. Dielectric constants $\epsilon_{r1}$ and $\epsilon_{r2}$ were fixed at 3.38 and 1 respectively, while the top substrate layer height $h_1$ was set to 0.813 mm.[5] Simulations were carried out at 10 GHz. Three values of bottom layer height, or back plane distance, were considered, namely $h_2 = \infty$, $\lambda_0$/4, and $\lambda_0$/6 (at 10 GHz, $\lambda_0/4 = 7.5$ mm and $\lambda_0/6 = 5$ mm). The case $h_2 = \infty$ is equivalent to the absence of a back plane, while an $h_2$ value of $\lambda_0$/6 was used in an earlier successful implementation on the present substrate of an 8-element uniform linear CPW-fed array [36]. A CPW feed line was designed for the case $h_2 = \infty$ by adjusting the centre strip width $w$ and slot width $s$ to yield a characteristic impedance of about 50 Ω (end values of $w$ and $s$ were 3.7 mm and 0.2 mm respectively). Adding a back plane at $\lambda_0$/4 and $\lambda_0$/6 had negligible effect on the characteristic impedance; hence the same $w$ and $s$ values were used throughout.

For each of the cases $h_2 = \infty$, $\lambda_0$/4, and $\lambda_0$/6, an isolated (radiating) slot with a width $W$ of 0.4 mm was designed to be resonant at 10 GHz by appropriately adjusting its half-length $L$. The resulting resonant slot half-lengths were 10.56 mm, 10.80 mm and 10.87 mm respectively, with corresponding self-impedances of 12.5 Ω, 11.2 Ω, and 13.9 Ω.

Subsequently, the mutual admittance $Y_{21}$ between broadside twin slots as in Fig. 4.1 was

[4] Results presented in Section 4.3 were published in [43].
[5] As noted previously, a higher dielectric constant has to be chosen for the top substrate layer than for the bottom layer in order to help achieve a non-leaky transmission line.

computed as a function of inter-slot distance $d$ for each instance of $h_2$. Slot dimensions were the same as those of the isolated resonant slot corresponding to the same $h_2$ (described above). The range of $d$ was $0.9\lambda_{CPW} \leq d \leq 3\lambda_{CPW}$ ($\lambda_{CPW}$ is the CPW wavelength at 10 GHz). Lengths $l_f$ of feed lines were $0.5\lambda_{CPW}$, equivalent to referring two-port network parameters to the centres of radiating slots ($\lambda_{CPW}$ is the CPW wavelength at 10 GHz).

### 4.3.3 Results

Fig. 4.17 shows the real and imaginary parts $g_{21}$ and $b_{21}$ of the normalized mutual admittance $y_{21}$ as a function of normalized distance $d/\lambda_{CPW}$ for each of the three cases $h_2 = \infty$, $\lambda_0/4$, and $\lambda_0/6$. $y_{21}$ is the mutual admittance $Y_{21}$ normalized with respect to the relevant isolated resonant slot self-admittance. Similar to Section 4.2, the reason for normalizing $Y_{21}$ is that, in a linear (uniform) array context, the relative size of mutual admittance magnitudes with respect to the slots' self-admittance magnitudes can be viewed as an indicator of the extent of the effect of mutual coupling on the array input impedance (*cf.* Section 1.1).

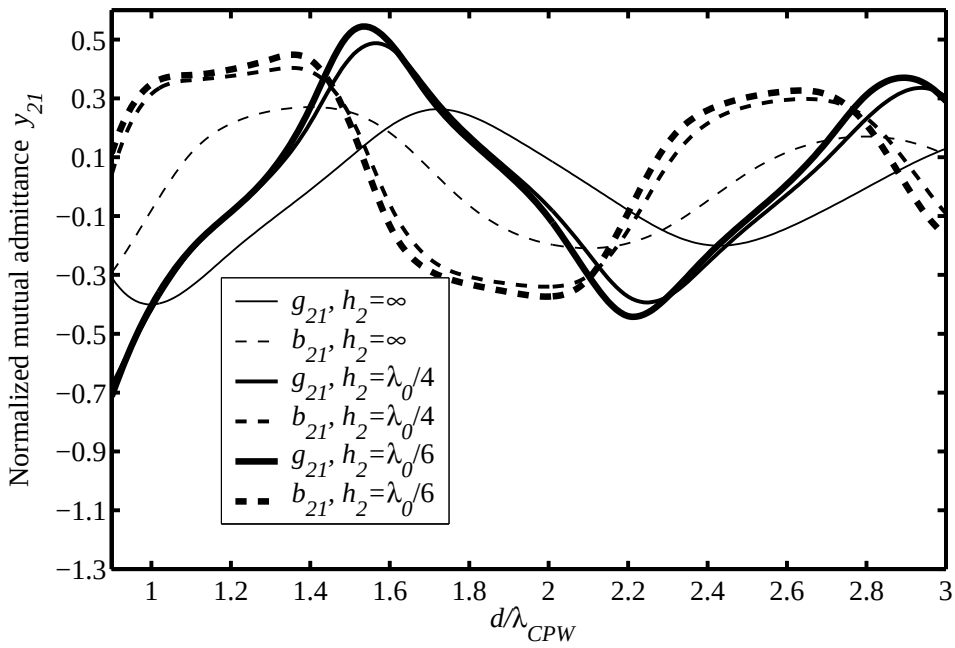


FIGURE 4.17: Real and imaginary parts $g_{21}$ and $b_{21}$ of normalized mutual admittance $y_{21}$ against interslot distance $d/\lambda_{CPW}$ at 10 GHz. $W$ = 0.4 mm; $h_1$ = 0.813 mm; $\epsilon_{r1}$ = 3.38; $\epsilon_{r2}$ = 1.

The normalized curves indicate that, in the absence of a back plane, the maximum values of the magnitudes of the real part ($G_{21}$) and imaginary part ($B_{21}$) of the mutual admittance $Y_{21}$ are about 40% and 27% respectively of the resonant slot self-admittance; the maximum of $|g_{21}|$ occurs at $d = \lambda_{CPW}$ and the maximum of $|b_{21}|$ at $d = 1.4\lambda_{CPW}$. Adding a back plane at $h_2 = \lambda_0/4$ results in significantly higher relative maximum values of about 68% and 40% for $|G_{21}|$ and $|B_{21}|$ respectively;

other extrema also show notable increases compared to the $h_2 = \infty$ case. The back plane has the effect of shifting the curves for $g_{21}$ and $b_{21}$ so that their extrema in general are not aligned with those of the curves for $h_2 = \infty$. These effects can be ascribed to internal mutual coupling (the external equivalent problem, concerned with fields in the half-space adjacent to the CPW ground planes, is unchanged by the addition of a back plane), indicating that the input impedance of an array on the single-layer substrate potentially could be significantly affected when a back plane is placed $\lambda_0/4$ away.[6] Decreasing the back plane distance to $h_2 = \lambda_0/6$ results in curves quite similar to, and more or less "in phase" with, the curves for the case $h_2 = \lambda_0/4$ with somewhat higher maximum values for $g_{21}$ and $b_{21}$ (0.71 and 0.45 respectively against 0.68 and 0.4). At $d = \lambda_{CPW}$ the magnitude of the real part of the mutual admittance was about 40% of the relevant resonant slot self-admittance for all cases of $h_2$.

In order to evaluate IE3D's performance with respect to computation of the mutual admittance curves of Fig. 4.17, $S_{21}$ as a function of frequency was computed for a specific instance of each of the cases $h_2 = \infty$ and $h_2 = 5$ mm ($\lambda_0/6$ at 10 GHz) which corresponded to an inter-slot distance of 20.35 mm ($0.95\lambda_{CPW}$ at 10 GHz; the relevant values of $y_{21}$ can be read from Fig. 4.17). $S_{21}$ against frequency was also measured for manufactured versions of these two test cases. Fig. 4.18 shows good agreement between computed and measured results for $|S_{21}|$, both with and without the back plane.

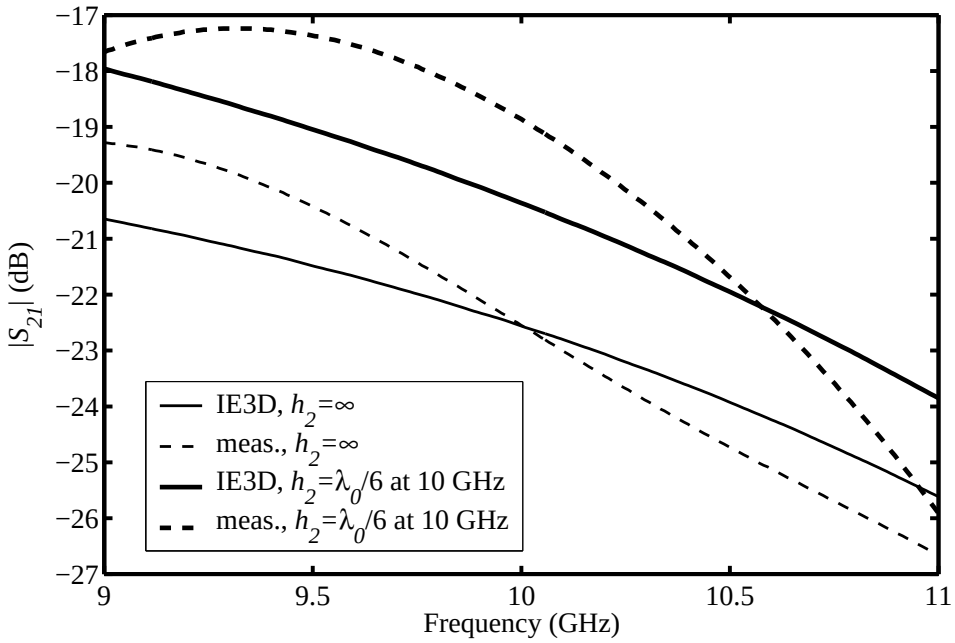


FIGURE 4.18: Computed and measured $|S_{21}|$ against frequency for twin slots spaced $d = 20.35$ mm apart (0.95 $\lambda_{CPW}$ at 10 GHz) on conductor-backed two-layer substrate for back plane distances $h_2 = \infty$ and $h_2 = 5$ mm ($\lambda_0$/6 at 10 GHz). $W$ = 0.4 mm; $h_1$ = 0.813 mm; $\epsilon_{r1}$ = 3.38; $\epsilon_{r2}$ = 1.

[6] The array's input impedance would of course ultimately be determined by the effect of the back plane on slot self-admittance values as well (*cf.* Eqs. (1.3) and (1.4)).

### 4.3.4 Conclusions

The effect of back plane distance on the normalized mutual admittance between CPW-fed slots on conductor-backed two-layered substrates was investigated. For the substrate under consideration, a back plane at a distance of $\lambda_0/4$ yielded curves of normalized mutual admittance against separation distance with substantially higher maxima and minima compared to the case where no back plane was present. A back plane distance of $\lambda_0/6$ produced normalized mutual admittance curves that were very similar in shape to those for the case $h_2 = \lambda_0/4$, but with somewhat larger maxima and minima, suggesting that the effect of mutual coupling increases as back plane distance decreases.